MICROBIOLOGY

Extremely low-frequency magnetic fields affect the movement of magnetotactic cocci

Roger Duarte de Melo[1], Natalia Belova[2], and Daniel Acosta-Avalos[1]

[1]Brazilian Center for Physics Research, Botafogo, 150, Rio de Janeiro, 22290–180, Brazil
[2]Institute of Theoretical and Experimental Biophysics of the Russian Academy of Sciences, ul. Institutskaya, 3, Pushchino, Moscow Oblast, 142290, Russian Federation

Address correspondence and requests for materials to Daniel Acosta-Avalos, dacosta@cbpf.br

Abstract

Magnetotactic bacteria are microorganisms that swim following the geomagnetic field lines, because of an intracellular magnetic moment that aligns their body to the magnetic field lines. For that reason, these bacteria are appropriate for the study of microorganisms' motion. The present paper studies the swimming trajectories of uncultured magnetotactic cocci under the effect of combined constant (DC) and alternating (AC) magnetic fields oscillating at frequencies that formally correspond to the cyclotron frequency for Ca^{2+}, K^{+}, Fe^{2+} and Fe^{3+} ions. The swimming trajectories were observed to be cylindrical helixes and their helix radiuses, frequencies, axial velocities and orientation angles of the trajectories relative to the constant magnetic field were determined. The orientation angles were used to calculate the magnetic to thermal energy ratio, which helps the study of the disorientating effect of the flagellar motion. Our results show that combined magnetic fields tuned to the resonance of Ca^{2+} ions affect all the trajectory parameters. Frequencies associated to Ca^{2+} and K^{+} do not affect the bacterial swimming direction relative to the magnetic field direction. On the other hand, frequencies associated to Fe^{2+} and Fe^{3+} do change the bacterial swimming direction relative to the magnetic field direction, which means that those frequencies affect the flagellar function. These results show indirect evidence of the action of calcium binding proteins in the motility of magnetotactic cocci.

Keywords: magnetotaxis, magnetotactic cocci, Ion Parametric Resonance model, Ion Cyclotron Resonance model, calcium-binding proteins, sheath-associated protein.

Citation: De Melo, R. D., Belova, N., and Acosta-Avalos, D. 2024. Extremely low-frequency magnetic fields affect the movement of magnetotactic cocci. Bio. Comm. 69(2): 69–75. https://doi.org/10.21638/spbu03.2024.202

Authors' information: Roger Duarte de Melo, PhD Student, orcid.org/0009-0006-7743-2081; Natalia Belova, PhD, Researcher, orcid.org/0009-0002-1751-0616; Daniel Acosta-Avalos, PhD, Researcher, orcid.org/0000-0002-5784-754X

Manuscript Editor: Andrey Plotnikov, Institute for Cellular and Intracellular Symbiosis, Ural Branch of the Russian Academy of Sciences, Orenburg, Russia

Received: October 20, 2023;

Revised: January 18, 2024;

Accepted: February 26, 2024.

Ethics statement: This paper does not contain any studies involving human participants or animals performed by any of the authors.

Competing interests: The authors have declared that no competing interests exist.

Introduction

The effect of very low frequency oscillating magnetic fields on living beings has been observed in several organisms and in different conditions (Krylov and Osipova, 2023). The frequencies observed to affect living beings have been related to resonance frequencies of ions such as calcium and potassium (Liboff, 2019). The first model to explain that effect was proposed by A. R. Libbof (1985) and is known as Ion Cyclotron Resonance (ICR) model. The ICR model assumes that to observe the effect, the magnetic field frequency must be the cyclotron frequency of the affected ion, independent of the magnitude of the oscillating magnetic field. However, the ICR model is not realistic for the typical dimension of a cell (Sandweiss, 1990). After Libbof, another model was proposed by V. V. Lednev (1991 and 1996), which is known as Ion Parametric Resonance (IPR) model. In this model, the observed effects are related to the interference between the vibrational states of an ion linked to a protein (considering the ion as a charged spatial oscillator). The vibrational ground state is split by the presence of a static magnetic field B_{DC}, and the interference of both states determines the probability to observe any bioeffect by an oscillating magnetic field B_{AC}. In other words, combined magnetic fields (CMF) generated by parallel magnetic fields B_{DC} and B_{AC}, can affect the

vital functions of living organisms through their effect on ions bound to proteins. The IPR model assumes that sinusoidal magnetic fields B_{AC} oscillating at the cyclotron frequency associated to a particular ion molecule, and determined by the magnetic field B_{DC}, can affect the biological function of the protein associated to that ion (Krylov and Osipova, 2023). The model assumes that $B = B_{DC} + B_{AC}{}^{*}\sin(2\pi f_C t)$, and to observe the bioeffect the following must be satisfied (Belova and Panchelyuga, 2010):

$$f_C = (q^{*}B_{DC}) / (2\pi m) \quad (1a)$$

$$B_{AC} = 1.8^{*}B_{DC} \quad (1b)$$

where q is the ion electric charge and m is the ion mass. The most common studied ions are Ca^{2+}, K^{+} and Mg^{2+} because of their biological importance. The use of appropriate CMFs can show the influence of Ca^{2+} on the motility and swimming of microorganisms (Smith, McLeod, Liboff, and Cooksey, 1987).

Magnetotactic bacteria (MTB) are microaerobic or anaerobic prokaryotes that biomineralize magnetic nanoparticles involved by a membrane and organized in linear chains in the cytoplasm (Abreu and Acosta-Avalos, 2018). The magnetic nanoparticles have been shown to be of magnetite (Fe_3O_4) or greigite (Fe_3S_4), both ferrimagnetic minerals. The set formed by the magnetic nanoparticle and the membrane is known as magnetosome. The magnetosome chain confers a magnetic moment to the MTB body, and through a magnetic torque with the external magnetic field, the MTB body swims oriented to the magnetic field lines, a property known as magnetotaxis (Esquivel and Lins de Barros, 1986; Kalmijn, 1981). As the local magnetic field changes its direction, the MTB present in the environment change their swimming direction accordingly to follow the new magnetic field direction. That property makes MTB a good model to study microorganism motion.

The aim of the present research was to investigate the movement and trajectory of uncultured MTB cocci under the presence of extremely low frequency oscillating magnetic fields and observe the influence of those magnetic fields on the bacterial trajectory parameters. For that, the movement was studied in the presence of CMFs tuned to the cyclotron frequency of Ca^{2+} and other ions as proposed by the IPR model.

Materials and methods

Non-cultured MTB cocci were collected in the Rodrigo de Freitas lagoon located in Rio de Janeiro, RJ, Brazil. The sediments with MTB cocci were collected in 2007 and stored in a glass aquarium. These magnetotactic cocci belong to the class Etaproteobacteria (Lin et al., 2018). The local geomagnetic parameters in Rio de Janeiro are: horizontal component = 0.18 Oe, vertical component = –0.15 Oe; total intensity = 0.23 Oe. As these MTB cocci are from South America, they are south-seeking, which means that their swimming direction is contrary to the magnetic field direction (Blakemore and Frankel, 1981).

Fig. 1. A — Glass microscope slide with a pair of coils to generate the magnetic field B_{DC}. The optical plane is on the glass surface and corresponds to the X — Z plane while the positive Y-axis points up. B — Experimental set-up. The digital microscope Celestron is inside a pair of coils used for the generation of the magnetic field B_{AC}. The microscope slide of figure A is fixed on the microscope stage; observe that both coil axes are parallel.

To isolate the MTB cocci for the experiments, sediments with water were transferred to a glass flask containing a lateral capillary aperture, and the MTB cocci were attracted to this capillary aperture using a small magnet that generated a magnetic field aligned to the capillary aperture (Lins et al., 2003). Samples were collected with a micropipette after 2 minutes.

For the trajectory analysis the movement of MTB cocci was recorded using a digital microscope (model 44340, Celestron, USA) with a pair of hand-made coils attached to a microscope slide (Fig. 1A), producing static (DC) magnetic fields perpendicular to the microscope optical axis (horizontal plane). A 10X lens was used together with a digital amplification of 4 times to observe the cocci. The movement was recorded in videos at 10 fps. A second pair of coils was used to generate the AC magnetic field. The digital microscope was inside the second pair of coils (Fig. 1B). The axis of the second pair of coils was parallel to the axis of the pair of coils attached to the microscope slide, guaranteeing the parallelism of the AC and DC magnetic fields. The AC magnetic field was generated by a sinusoidal voltage provided by a function generator (model 33250A, Agilent, USA) connected to the second pair of coils. The magnetic field generated by each coil was measured using a 3-axis fluxgate magnetometer (model 113, Applied Physics Systems, USA). The magnetometer permitted to confirm that both magnetic fields (the applied DC magnetic field and the AC magnetic field) were parallel and perpendicular to the geomagnetic field. Control experiments were recorded with B_{DC} only ($B_{AC} = 0$). Combined experiments were conducted with B_{DC} and B_{AC} together. In both cases, a drop of water was collected from the concentrator capillary aperture using a micropipette and put on the microscope slide with B_{DC} already turned on. The movement video started when MTB cocci were accumulated in the drop border. The MTB cocci started their movement when the direction of B_{DC} was inverted, because of the inversion of the current direction in the coils. A drop of water was used to record only a pair of Control and Combined experiments, always in that order, and a new drop was used to record a new pair of experiments. For each experimental condition there were used enough number of drops to get about 40 trajectories.

For the experiments the microscope was oriented so as to make the geomagnetic field perpendicular to the CMF. In other words, if the XZ plane corresponds to the focal plane and the Y axis is the vertical axis, then: $\boldsymbol{B}_{CMF} = (B_{DC} + B_{AC}{}^{*}\sin(2\pi f_C t))\,\mathbf{k}$ and $\mathbf{B}_{GEO} = (0.18\ \text{Oe})\,\mathbf{i} + (0.15\ \text{Oe})\,\mathbf{j}$, where **i**, **j**, **k** are the Cartesian unit vectors. Table 1 shows the values for B_{DC}, B_{AC} and the cyclotron frequency f_c chosen for ions Ca^{2+}, K^{+}, Fe^{2+} and Fe^{3+} according to Eqs. (1). We chose Ca^{2+} and K^{+} because of their importance in cellular functions (Belova and Panchelyuga, 2010) and Fe^{2+} and Fe^{3+} because of their high presence in MTB to produce magnetosomes.

Table 1. Values of B_{DC}, B_{AC} and f_C used to generate the CMF associated to each ion resonance. The values of B_{DC} and f_C were obtained from Eqs. 1

Ion	B_{DC} (Oe)	B_{AC} (Oe)	f_C (Hz)
Ca^{2+}	0.59	1.06	45.2
K^{+}	0.72	1.29	28.2
Fe^{2+}	0.66	1.18	36.2
Fe^{3+}	0.57	1.03	47.3

The values for B_{AC} were limited by the maximum value of B generated by the set of coils at the frequency f_C, keeping the AC voltage amplitude in the function generator at 10 Volts.

Video records were analyzed with the *ImageJ* software (NIH, USA). Trajectory coordinates were obtained manually frame by frame for each microorganism and later analyzed with the software *MicroCal Origin*. It is known that the set of coordinates of X and Z (see below) of the experimental bacterial trajectories are plane projections of cylindrical helixes. For each trajectory the translational velocity V_T, the helix frequency *f* and the helix radius R were estimated. Statistical tests were performed with the software *GraphPad InStat*, and the angular statistics were performed with the software *Oriana* 4.02.

Parametrization of bacterial trajectories

Bacterial movement occurs under the low Reynolds' number regime. One consequence is that the bacterial trajectory is a cylindrical helix (Crenshaw, 1996; Nogueira and Lins de Barros, 1985), whose equations as a function of time are:

$$x(t) = R^{*}\cos(\omega t) \quad (2a)$$

$$y(t) = R^{*}\sin(\omega t) \quad (2b)$$

$$z(t) = V^{*}t \quad (2c)$$

where the Z axis coincides with the helix axis, V is the axial velocity, R is the helix radius, $w = 2pf$ is the angular velocity and f is the helix frequency.

The bacteria swimming recorded in a microscope produces bidimensional data (Fig. 2). Considering the Z axis parallel to the helix axis and located on the focal plane together with the X axis, the trajectory observed must be a waving line with parametric equations (2a) and (2c). When the helix axis does not coincide with the Z axis but is inclined by an angle θ, the parametric equations for the coordinates z and x transform as follows:

$$x' = -z^{*}\sin\theta + x^{*}\cos\theta = \\ = -R^{*}\cos\theta^{*}\cos(2\pi ft) + V^{*}t^{*}\sin\theta \quad (3a)$$

$$z' = z^{*}\cos\theta + x^{*}\sin\theta = \\ = R^{*}\sin\theta^{*}\cos(2\pi ft) + V^{*}t^{*}\cos\theta \quad (3b)$$

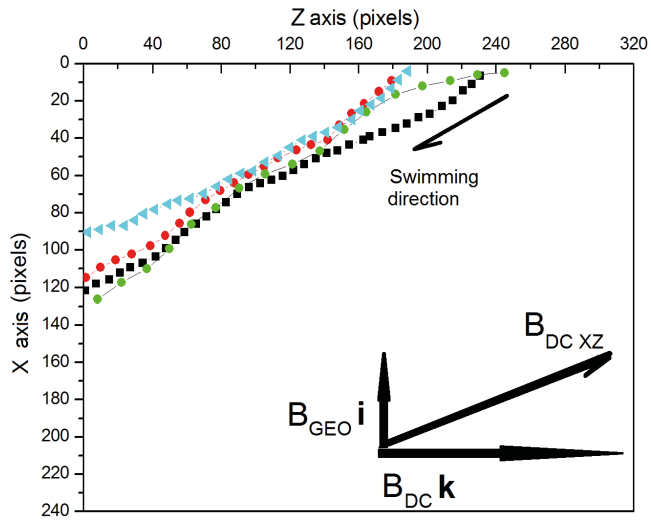

Fig. 2. Example of MTB trajectory curves. The axis' orientation is the same as in the microscope display. The arrow below the trajectories represents the swimming direction. The magnetic fields $B_{GEO\ X}$ and B_{DC} and the total B_{DCXZ} are also shown. Observe that the swimming direction is contrary to the direction of B_{DCXZ} because the studied magnetotactic cocci are south-seeking.

Eqs. 3a and 3b represent a straight line plus a sinusoidal waving. The angle q results from the misalignment among the helix axis and the magnetic field lines because of thermal perturbations. Experimentally, the inclination angle θ and the trajectory parameters V, R and *f* can be calculated using Eqs. (3a) and (3b). To perform good experimental adjustments the helix axis which coincides with the magnetic field lines must be parallel to some frame axis (horizontal or vertical) in the video. To this purpose, the position of the camera was adjusted so that the horizontal axis of each frame was aligned to the DC applied magnetic field.

Results and discussion

Magnetotactic cocci swim in trajectories that can be adjusted as cylindrical helixes (Fig. 2). As the DC magnetic field has two components in our experimental setup, the resultant DC magnetic field is composed by the applied DC magnetic field and the geomagnetic field: $\mathbf{B}_{DC\ Total}$ = (0.18 Oe) **i** + (0.15 Oe) **j** + B_{DC}**k**.

Our results show that the combined magnetic field does not affect the magnetotactic behavior compared to the control experiments, since in all experimental conditions MTBs respond to the magnetic field direction change.

Table 2 shows the parameters V, R and *f* calculated for MTB trajectories. We observe that the frequency associated to Ca^{2+} produces a statistically significant increase in the velocity (Student t-test, p = 0.02) and trajectory radius (Student t-test, p = 0.001), and that the frequency associated to Fe^{3+} produces a statistically significant decrease only in the velocity (Student t-test, p = 0.02). The effects of CMF tuned to Ca^{2+} frequency on the trajectory parameters show indirectly that the flagellar function of these MTB coccus is associated to calcium dependent proteins.

Table 2. Parameters of the MTB trajectories. The values of the parameters V, R and *f* for the helicoidal trajectories, in the presence of CMF, were obtained from data analysis using Eqs. 3

	V ± SD (μm/s)	R ± SD (μm)	*f* ± SD (Hz)	N
Ca^{2+}				
Control	89 ± 41.7	2.43 ± 1.69	1.01 ± 0.73	43
Experiment	101.9 ± 37.1	3.89 ± 2.57	0.76 ± 0.36	42
t-test	s. (p = 0.02)	s. (p = 0.001)	s. (p = 0.05)	
K^{+}				
Control	82.7 ± 20.5	2.46 ± 1.59	0.98 ± 0.56	48
Experiment	99.9 ± 43.8	2.56 ± 1.53	0.95 ± 0.43	43
t-test	n. s.	n. s.	n. s.	
Fe^{2+}				
Control	89.4 ± 33	2.65 ± 1.54	0.84 ± 0.55	40
Experiment	79.1 ± 27.4	3.63 ± 2.99	0.74 ± 0.35	40
t-test	n. s.	n. s.	n. s.	
Fe^{3+}				
Control	131.4 ± 33.2	4.05 ± 2.43	1.08 ± 0.41	38
Experiment	113.6 ± 32.5	4.2 ± 2.39	1.06 ± 0.5	41
t-test	s. (p = 0.02)	n. s.	n. s.	

SD means standard deviation and N is the number of analyzed trajectories. Control corresponds to $B_{AC} = 0$ and Experiment corresponds to the presence of CMF ($B_{AC} \neq 0$). Each pair of Control and Combined results was compared using a Student t-test: n. s. means not significant (p > 0.05) and s. means significant (p < 0.05).

Another movement parameter is the trajectory orientation relative to the applied DC magnetic field. Magnetotaxis is recognized because magnetotactic microorganisms react to changes in the magnetic field direction, swimming in trajectories parallel to the magnetic field direction (Fig. 2). In our experiments magnetotactic microorganisms do not react to the AC magnetic field and follow only the resultant DC magnetic field. As the axial velocity has the same direction as the helicoidal trajectory axis, the components of the axial velocity were used to determine the trajectory angle θ relative to the Z axis because the main DC magnetic field component is on this axis and q corresponds to the angle among the axial velocity and B_{DC}. The angle θ was calculated using Eqs. (3), the expected angle θ_{MF} was calculated as arctan (B_{GEO}/B_{DC}) and the results are shown in Table 3. It can be observed that MTB coccus swim following the direction of the total DC magnetic field ($\mathbf{B}_{DC\ Total}$), as expected for magnetotactic behavior (Frankel and Blakemore, 1980).

Table 3. Circular statistics for trajectory angles θ (the angle between the axial velocity and the magnetic field BDC)

	θ ± SD (deg)	θ_{MF}(deg)
Ca^{2+}		
Control	24.3 ± 5.9	22
Experiment	24.2 ± 5	
K^+		
Control	19.2 ± 5.8	18
Experiment	19.6 ± 4.1	
Fe^{2+}		
Control	22 ± 4.6	19
Experiment	23.6 ± 8.1	
Fe^{3+}		
Control	25.1 ± 7.5	22
Experiment	20.5 ± 11.6	

SD means Circular Standard Deviation. Control corresponds to $B_{AC} = 0$ and Experiment corresponds to the presence of CMF ($B_{AC} \neq 0$). θ_{MF} corresponds to the angle between the total DC magnetic field ($B_{GEO} + B_{DC}$) and the Z axis. For all the angle groups (Control and Experiment) the Rayleigh test gives $p << 0.05$, meaning that the angles are not distributed uniformly around the circle but are concentrated around the mean angle. Comparison among groups of angles Control and Experiment was done using the Watson-William F-test and in all the cases the mean angles are not significantly different ($p > 0.05$).

Table 4. Circular statistics for relative angles $\theta_{REL} = \theta - \theta_{MF}$

	Mean θ_{REL}	SD	r	Concentration
Ca^{2+}				
Control	2.8	5.9	0.995	91.7
Experiment	2.6	5	0.996	131.7
K^+				
Control	1.7	5.8	0.995	99.4
Experiment	2.1	4.1	0.997	194
Fe^{2+}				
Control	3.5	4.6	0.997	156.5
Experiment	5.2	8.1	0.99	50.1
Fe^{3+}				
Control	3.6	7.5	0.991	58.7
Experiment	359	11.7	0.979	24.6

SD means Circular Standard Deviation. Control corresponds to BAC = 0 and Experiment corresponds to the presence of CMF (BAC ≠ 0). r corresponds to the mean vector length and $0 < r < 1$. The concentration is a parameter that measures how the angles are distributed around the mean value: higher concentration values mean all the angles are very close to the mean angle. The angle groups (Control and Experiment) are not distributed uniformly around the circle but are concentrated around the mean angle (Rayleigh test $p << 0.05$). Comparison between groups of the angles Control and Experiment was done using the Watson — William F-test; for Ca^{2+}, K^+ and Fe^{2+} the mean angles are not significantly different ($p > 0.05$) and for Fe^{3+} there is a tendency to control and experiment angles be statistically different ($p = 0.05$).

Table 4 shows the circular statistics for the relative angles $\theta_{REL} = \theta - \theta_{MF}$ used to get insights about the effect of B_{AC} on the magnetotactic behavior. It can be seen that frequencies associated to Ca^{2+} and K^+ do not change the mean angle (Watson — Williams F-test: $p > 0.05$). For the frequencies associated to Fe^{2+} and Fe^{3+} the mean angles tend to be statistically different only for Fe^{3+} (Watson — Williams F-test: $p = 0.05$), the standard deviation increases for both frequencies when compared to the control and, consequently, the concentration of angles around the mean value decreases, meaning that these frequencies affect the magnetotactic behavior.

These results show that frequencies associated to Ca^{2+} and K^+ do not affect the MTB swimming direction relative to the magnetic field direction, and that frequencies associated to Fe^{2+} and Fe^{3+} affect the MTB swimming direction relative to the magnetic field direction. This direction is determined by the action of flagellar and magnetic torques, meaning that for so far unknown reasons the Fe^{2+} and Fe^{3+} frequencies change the flagellar torque in such a way that oppose to the orientating effect of the magnetic torque. Another way to observe this is to calculate the magnetic to thermal energy ratio (X = mB/kT), through the calculation of the mean value of $\cos\theta_{REL}$ and its variance σ^2, as in Acosta-Avalos et al. (2019), De Melo, Leão, Abreu and Acosta-Avalos (2020) and Carvalho, Abreu and Acosta-Avalos (2021). Briefly, Kalmijn (1981) showed that the average value for $\cos\theta_{REL}$ ($<\cos\theta_{REL}>$) follows the Langevin function with X as argument and calculated the variance of $\cos\theta_{REL}$:

$$<\cos\theta_{REL}> = \coth(X) - 1/X \quad (4a)$$

$$\sigma^2 = 1 - \coth^2(X) + 1/X^2 \quad (4b)$$

Using Eqs (4) it is easy to isolate X to get the following expression:

$$X = 2<\cos\theta_{REL}> / (1 - <\cos\theta_{REL}>^2 - \sigma^2) \quad (5)$$

Table 5 shows the values of X for all the experimental conditions. As can be seen, for Ca^{2+} and K^+, X increases when compared to the control experiment, which means that in those conditions the flagella improve its function, decreasing the disturbing effective temperature associated to the disorientating thermal energy. On the other hand, for Fe^{2+} and Fe^{3+} the value of X decreases when compared to the control experiment, which means that the effective temperature increases through some sort of flagellar malfunction that disorients the MTB swimming direction.

Table 5. Statistics of $\cos\theta_{REL}$

	$\langle\cos\theta_{REL}\rangle$	Variance	$X = mB/k_BT$
Ca^{2+}			
Control	0.993	2.6×10^{-4}	151.9
Experiment	0.995	3.4×10^{-5}	208.7
K^+			
Control	0.995	1×10^{-4}	183.3
Experiment	0.997	5.2×10^{-5}	308.4
Fe^{2+}			
Control	0.995	3.7×10^{-5}	198.1
Experiment	0.986	5.5×10^{-4}	72.2
Fe^{3+}			
Control	0.989	2.5×10^{-4}	96.3
Experiment	0.979	2.5×10^{-3}	51.1

The average value of $\cos\theta_{REL}$ is represented as $\langle\cos\theta_{REL}\rangle$. σ^2 is the variance for the different sets of $\cos\theta_{REL}$. X is the magnetic to thermal energy ratio (X = mB/kT), where m is the magnetic moment, T is the absolute temperature, k is the Boltzmann constant and B is the applied magnetic field. Control corresponds to $B_{AC} = 0$ and Experiment corresponds to the presence of CMF ($B_{AC} \neq 0$). As Carvalho et al. (2021) show, the magnetic moment for this magnetotactic cocci is about 8×10^{-15} Am^2, producing $X \approx 147$ for B = 0.7 Oe. The values of X for control experiments are in accordance with that value.

Our experiments with combined magnetic fields show that Ca^{2+} is related to the movement in MTB coccus, as has been shown in other MTB (Lefevre et al., 2010). The increase in velocity and improvement in swimming direction relative to the DC magnetic field in the presence of resonant conditions for Ca^{2+} can be understood as an improvement in motility, as has been shown in diatoms *Amphora coffeaeformis* (Smith, McLeod, Liboff, and Coosey, 1987). This result is evidence of the involvement of calcium-dependent proteins in the motility of our uncultured magnetotactic cocci. It has been shown that the sheath enclosing the flagellar bundle from the MO-1 marine MTB culture consists of a glycoprotein named sheath-associated protein (sap), homologous to eukaryotic calcium-dependent adherent proteins (cadherin). In the MO-1 MTB culture calcium ions mediate the assembly of the tubular-shaped sheath, which is essential for MTB swimming (Lefevre et al., 2010). On the other hand, the effect of Fe^{2+} and Fe^{3+} frequencies as observed here has never been reported. Khokhlova et al. (2018) investigated the metabolism of the bacterium *Rhodospirillum rubrum* under the presence of AC and DC magnetic fields in resonance conditions for phosphorous and Fe^{3+}. They observed that the consumption of nitrate and iron in the culture medium increased under the presence of the combined magnetic fields. As far as we know, there is no reported protein binding iron associated to flagella described for magnetotactic microorganisms. We do not expect that the effect is caused by magnetosomes because magnetotaxis is not disrupted, but the high content of intracellular iron in these microorganisms makes it possible to consider that proteins binding iron are also involved in the flagellar function.

It is interesting to consider that magnetotactic bacteria can be influenced by natural oscillating magnetic fields combined with the static geomagnetic field. However, the amplitudes of those natural oscillating magnetic fields are too small when compared to the amplitude of the geomagnetic field (Palmer, Rycroft, and Cermack, 2006), and do not satisfy the condition showed in Eq. 1b. The results shown here can be observed only in laboratory and help us to understand the participation of intracellular ions in the bacterial movement.

Conclusion

The present manuscript shows that experiments with combined DC and AC magnetic fields at low frequencies tuned to the resonance of Ca^{2+} ions, following the Ion Parametric Resonance model, produce direct evidence of the influence of calcium in the motility of MTB and indirect evidence of the participation of calcium binding proteins in their flagellar system. When the combined magnetic field is tuned to the resonance of Fe^{2+} and Fe^{3+} the effects observed can be understood as evidence of iron binding proteins participating in the flagellar function. These last results were never reported in MTB and deserve future studies. The experiments with resonance frequencies tuned to K^+ show that the mere presence of AC magnetic field does not affect the bacterial movement, but it is necessary for the frequency to be associated with the cyclotron frequency of ions influencing the bacterial flagellar system.

Acknowledgements

R. D. de Melo thanks National Council for Scientific and Technological Development (CNPq) for PIBIC grant. We acknowledge Dr. Michel Spira from Minas Gerais Federal University UFMG for reading the manuscript and correcting the English grammar and style.

References

Abreu, F. and Acosta-Avalos, D. 2018. Biology and physics of magnetotactic bacteria; pp. 1–19 in Blumenberg, M., Shaaban, M., Elgaml, A. (eds), *Microorganisms.* 1st ed. IntechOpen, London.

Acosta-Avalos, D., Figueiredo, A. C., Conceição, C. P., da Silva, J. J. P., Aguiar, K. J. M. S. P., Medeiros, M. L., Nascimento, N., de Melo, R. D., Sousa, S. M. M., Lins de Barros, H., Alves, O. C., and Abreu, F. 2019. U-turn trajectories of magnetotactic cocci allow the study of the correlation between their magnetic moment, volume and velocity. *European Biophysics Journal* 48:513–521. https://doi.org/10.1007/s00249-019-01375-2

Belova, N. A. and Panchelyuga, V. A. 2010. Lednev's model: theory and experiment. *Biophysics* 55:661–674. https://doi.org/10.1134/S0006350910040263

Blakemore, R. P. and Frankel, R. B. 1981. Magnetic navigation in bacteria. *Scientific American* 245(6):58–65. https://doi.org/10.1038/scientificamerican1281-58

Carvalho, A. L., Abreu, F., and Acosta-Avalos, D. 2021. Multicellularity makes the difference: multicellular magnetotactic prokaryotes have dynamics motion parameters dependent on the magnetic field intensity. *European Physics Journal Plus* 136:203. https://doi.org/10.1140/epjp/s13360-021-01187-4

Crenshaw, H. C. 1996. A new look at locomotion in microorganisms: rotating and translating. *Amer Zool* 36(6):608–618. https://doi.org/10.1093/icb/36.6.608

De Melo, R. D., Leão, P., Abreu, F., and Acosta-Avalos, D. 2020. The swimming orientation of multicellular magnetotactic prokaryotes and uncultured magnetotacticcocci in magnetic fields similar to the geomagnetic field reveals diferences in magnetotaxis between them. *Antonie van Leeuwenhoek* 113:197–209. https://doi.org/10.1007/s10482-019-01330-3

Esquivel, D. M. S. and Lins de Barros, H. G. P. 1986. Motion of magnetotactic microorganisms. *Journal of Experimental Biology* 121(1):153–163. https://doi.org/10.1242/jeb.121.1.153

Frankel, R. B. and Blakemore, R. P. 1980. Navigational compass in magnetic bacteria. *Journal of Magnetism and Magnetic Materials* 15–18(3):1562–1564. https://doi.org/10.1016/0304-8853(80)90409-6

Kalmijn, A. J. 1981. Biophysics of geomagnetic field detection. *IEEE Transactions on Magnetics* MAG-17(1):1113–1124. https://doi.org/10.1109/TMAG.1981.1061156

Krylov, V. V. and Osipova, E. A. 2023. Effects of weak low-frequency magnetic fields: frequency-amplitude efficiency windows and possible mechanisms. *International Journal of Molecular Sciences* 24(13):10989. https://doi.org/10.3390/ijms241310989

Khokhlova, G., Abashina, T., Belova, N., Panchelyuga, V., Petrov, A., Abreu, F., and Vainshtein, M. 2018. Effects of combined magnetic fields on bacteria Rhodospirillum rubrum VKM B-1621. *Bioelectromagnetics* 39(6):485–490. https://doi.org/10.1002/bem.22130

Lednev, V. V. 1991. Possible mechanism for the influence of weak magnetic fields on biological systems. *Bioelectromagnetics* 12(2):71–75. https://doi.org/10.1002/bem.2250120202

Lednev, V. V. 1996. Bioeffects of weak combined, constant and variable magnetic field. *Biophysics* 41:241–252.

Lefevre, C. T., Santini, C. L., Bernadac, A., Zhang, W. J., Li, Y., and Wu, L. F. 2010. Calcium ion-mediated assembly and function of glycosylated flagellar sheath of marine magnetotactic bacterium. *Molecular Microbiology* 78(5):1304–1312. https://doi.org/10.1111/j.1365-2958.2010.07404.x

Liboff, A. R. 2019. ION cyclotron resonance: geomagnetic strategy for living systems? *Electromagnetic Biology and Medicine* 38(2):143–148. https://doi.org/10.1080/15368378.2019.1608234

Liboff, A. R. 1985. Geomagnetic cyclotron resonance in living cells. *Journal of Biological Physics* 13:99–102. https://doi.org/10.1007/BF01878387

Lin, W., Zhang, W., Zhao, X., Roberts, A., Paterson, G., Bazylinski, D., and Pan, Y. 2018. Genomic expansion of magnetotactic bacteria reveals an early common origin of magnetotaxis with lineage-specific evolution. *The ISME Journal* 12(6): 1508–1519. https://doi.org/10.1038/s41396-018-0098-9

Lins, U., Freitas, F., Keim, C. N., Lins de Barros, H., Esquivel, D. M. S., and Farina, M. 2003. Simple homemade apparatus for harvesting uncultured magnetotactic microorganisms. *Brazilian Journal of Microbiology* 34(2):111–116. https://doi.org/10.1590/S1517-83822003000200004

Nogueira, F. S. and Lins de Barros, H. G. P. 1985. Study of the motion of magnetotactic bacteria. *European Biophysics Journal* 24:13–21. https://doi.org/10.1007/BF00216826

Palmer, S. J., Rycroft, M. J., and Cermack, M. 2006. Solar and geomagnetic activity, extremely low frequency magnetic and electric fields and human health at the Earth's surface. *Surveys in Geophysics* 27:557–595. https://doi.org/10.1007/s10712-006-9010-7

Sandweiss, J. 1990. On the cyclotron resonance model of ion transport. *Bioelectromagnetics* 11(2):203–205. https://doi.org/10.1002/bem.2250110210

Smith, S. D., McLeod, B. R., Liboff, A. R., and Cooksey, K. 1987. Calcium cyclotron resonance and diatom motility. *Bioelectromagnetics* 8(3):215–227. https://doi.org/10.1002/bem.2250080302